



**HAL**  
open science

## Effect of temperature and initial state on variation of thermal parameters of fine compacted soils

Ahmed Boukelia, S. Rosin-Paumier, Hossein Eslami, Farimah Masrouri

► **To cite this version:**

Ahmed Boukelia, S. Rosin-Paumier, Hossein Eslami, Farimah Masrouri. Effect of temperature and initial state on variation of thermal parameters of fine compacted soils. *European Journal of Environmental and Civil Engineering*, 2017, 23 (9), pp.1125-1138. 10.1080/19648189.2017.1344144 . hal-01717778

**HAL Id: hal-01717778**

**<https://hal.science/hal-01717778>**

Submitted on 18 Jun 2018

**HAL** is a multi-disciplinary open access archive for the deposit and dissemination of scientific research documents, whether they are published or not. The documents may come from teaching and research institutions in France or abroad, or from public or private research centers.

L'archive ouverte pluridisciplinaire **HAL**, est destinée au dépôt et à la diffusion de documents scientifiques de niveau recherche, publiés ou non, émanant des établissements d'enseignement et de recherche français ou étrangers, des laboratoires publics ou privés.

1           **Effect of temperature and initial state on variation of thermal**  
2                           **parameters of fine compacted soils**

3  
4                   **Boukelia, A.<sup>1,2</sup>, Eslami, H.<sup>1,2</sup>, Rosin-Paumier, S.<sup>1,2\*</sup>, Masrouri, F.<sup>1,2</sup>**

5           <sup>1</sup> *LEMETA – CNRS UMR 7563, Université de Lorraine, Vandoeuvre-lès-Nancy, F-54500,*  
6           *France.*

7           <sup>2</sup> *ESITC de Metz, Metz, France*

8           \*Corresponding author: [sandrine.rosin@univ-lorraine.fr](mailto:sandrine.rosin@univ-lorraine.fr)

9  
10           Postal address: ESNG - LEMETA, Bâtiment E, 2 rue du Doyen Marcel Roubault, TSA 70605, 54518

11           Vandoeuvre-lès-Nancy, France

12           **Acknowledgements :**

13  
14           The authors acknowledge C. Fontaine from IC2MP laboratory (Poitiers, France) for the  
15           mineralogical analyses.

## 18 **1. Introduction**

19 Soil thermal properties are required in some engineering applications such as the design of  
20 high-level radioactive waste disposals (Rutqvist, Wu, Tsang, & Bodvarsson, 2002), buried  
21 power transmission (De Lieto Vollaro, Fontana, & Vallati, 2011), energy geostructures  
22 (Pahud, 2002 and Brandl, 2006) and thermal energy storage (Navarro et al., 2016 and  
23 Giordano, Comina, Mandrone, & Cagni, 2016 ). The study of heat flow in soil is based on the  
24 thermal properties and temperature gradient. The thermal parameters governing the transfer of  
25 heat are the **thermal conductivity** ( $\lambda$ ), which is the ability of the material to conduct heat, the  
26 **volumetric heat capacity** ( $C$ ), which describes the ability of the material to store thermal  
27 energy while undergoing a given temperature change, and the **thermal diffusivity** ( $\alpha = \lambda/C$ ),  
28 which describes the ability of a material to conduct thermal energy relative to its ability to  
29 store thermal energy.

30 A variety of measurement techniques are available for natural materials with a broad  
31 temperature range. Recently, Zhang, Cai, Liu & Puppala (2016) presented most commonly  
32 used measurement techniques such as the steady-state method, the transient hot-wire method,  
33 the laser flash diffusivity method and the transient plane source method. The hot-wire method  
34 also known as the needle-probe method (ASTM, 2000) is a transient technique that measures  
35 temperature rise at a known distance from a linear heat source embedded in the test sample.  
36 This method is widely used in natural soil and compacted soil characterization for its  
37 accuracy, speed and simple application.

38 The thermal parameters ( $\lambda$ ,  $C$  and  $\alpha$ ) depend on soil parameters such as the mineralogy, water  
39 content, bulk density, particle size distribution and structural arrangement (Abu-Hamdeh  
40 (2001), Abu-Hamdeh (2003), Tang (2005), Brandl (2006), Ehdezi (2012)). Abu-Hamdeh and  
41 Reeder (2000) measured the thermal conductivity of four soils as a function of their water  
42 content and density. The authors noted that for each soil,  $\lambda$  increased with increasing density.

43 Similarly, when the water content increased  $\lambda$ , increased as well. The results of Tang (2005)  
44 showed the same trends for a clayey material. Barry-Macaulay, Bouazza, Singh, Wang, and  
45 Ranjith (2013) presented the same type of results as part of their important database of  
46 Australian natural materials. For instance, as the thermal conductivity of solid particles  
47 exceeds those of the air and the water, an increase in the dry density results in an increase in  
48  $\lambda$ . Furthermore, increasing the contact surface between solid particles increases the heat flux  
49 and results in an increase of  $\lambda$ . In the same way, as the thermal conductivity of water is higher  
50 than that of the air, an increase in the saturation rate results in an increase in  $\lambda$ .

51 Few studies have been conducted on the thermal conductivity of compacted soils. Ekwue,  
52 Stone, and Bhagwat (2006) studied the combined effects of soil density and water content on  
53 soil thermal conductivity of three soils: a sandy loam, a clayey loam and a clay. They  
54 measured the thermal conductivity for different values of water content and dry density on the  
55 compaction curve of these soils. For each soil,  $\lambda$  reaches a maximal value near the Proctor  
56 optimum water content. The study of Ekwue et al. (2006) was also focused on the impact of  
57 soil mineralogy on  $\lambda$ , and the material with a high sand content showed the most important  
58 impact. However, the coupled effect of soil density and water content on the volumetric heat  
59 capacity and thermal diffusivity was not well studied. The monotonic and cyclic heat effect on  
60 thermal parameters was also not studied.

61 Several prediction models of soil thermal parameters, taking into account the soil properties,  
62 are available to evaluate the thermal conductivity (De Vries (1963), Johansen (1977) and  
63 Kersten (1949)). For example, Farouki (1981) and, more recently, Dong, John, McCartney,  
64 and Lu (2015) presented an extensive review of the numerous available prediction models.  
65 However, these models are perfectible (Dong et al. 2015) and need to be improved to take  
66 into account new environmental or industrial issues such as soil temperature.

67 In civil engineering, the temperature variation range evolves according to the process; for  
68 example, cyclic variations from 4 and 30°C were recorded for heat exchange piles (Peron,  
69 Knellwolf, & Laloui, 2011) a maximum temperature of 70°C was estimated for thermal  
70 energy storage (Giordano et al. 2016), 100°C was used for the design of high-level radioactive  
71 waste disposal (Tang, 2005), and 90°C was used in the design of buried power transmission  
72 cables (Hanna, Chikhani, & Salama, 1993). Temperature variations affect the physical  
73 properties of soil (solid and water particles volumetric variation and change in water status),  
74 inducing changes in the thermal properties. Considering the impact of temperature on the  
75 thermal proprieties of soils between 0° and 70°C, only a few studies are available. Hiraiwa  
76 and Kasubuchi (2000) measured the thermal conductivity of two soils, a clay loam and a light  
77 clay, at different volumetric water contents and different temperatures between 5 and 75°C.  
78 Their results showed that  $\lambda$  increased with increasing temperature and volumetric water  
79 content. Smits, Sakaki, Howington, Peters, and Illangasekare (2013) measured the thermal  
80 conductivity and diffusivity of two sands prepared at various saturation rates at different  
81 temperatures between 30 and 70°C. Their results showed that the thermal properties increased  
82 dramatically for temperatures above 50°C, but small changes in thermal properties were  
83 observed at temperatures between 30 and 50°C.

84 This literature review shows that numerous studies are available on the impact of soil  
85 parameters on the soil thermal conductivity; some of these studies address compacted soils,  
86 but fewer focus on the compacted soils used in civil engineering that are submitted to cyclic  
87 temperature variations from 1 to 70°C. Furthermore, few studies and little data are available  
88 on the variation of the volumetric heat capacity and the thermal diffusivity as a function of  
89 soil properties, despite their great importance in the study of heat flow and heat storage in  
90 soils.

91 The aim of this study was to better understand the coupled effect of water content ( $w$ ),  
92 dry density ( $\rho_d$ ) and temperature variations ( $T$ ) on the thermal parameters ( $\lambda$ ,  $C$  and  $\alpha$ ) of  
93 compacted soils. The following issues were addressed:

- 94 • whether the mineralogy and the size distribution of soil particles affect their thermal  
95 properties,
- 96 • the coupled effect of  $w$  and  $\rho_d$  on the thermal parameters, and
- 97 • the effect of monotonic and cyclic thermal variation on soil thermal characteristics.

98 In the following sections, the preparation of the materials and the experimental device are  
99 described first. Then, the results are presented and analysed to explain the main evolutions of  
100 the thermal properties according to the initial state parameters of compacted soils and the  
101 impact of thermal variations.

## 102 **2. Materials and methods**

103 In this section, the properties of the five studied materials, the compaction of the materials at  
104 various water contents and dry densities, and the apparatus used to measure the thermal  
105 properties are presented.

### 106 **2.1. The materials properties**

107 Five different soils were studied. The mineralogical compositions of these soils are presented  
108 in *Table 1*. The illitic soil (I) named Arginotech® came from eastern Germany. The Plaisir  
109 loam (PL) was extracted from the Paris region and was dried, pulverized and sieved through a  
110 2 mm sieve before being quartered and used for various experiments (Boukelia, 2016). Two  
111 other loams from the Parisian basin, namely, the Jossigny loam (JL) and the Xeuilley loam  
112 (XL), were also studied. The characteristics of each material including grain size distribution,  
113 Atterberg limits (AFNOR, 1993), specific surface (AFNOR, 1999a), carbonate content  
114 (AFNOR, 1996) and Proctor compaction parameters (AFNOR, 1999b) are listed in *Table 2*.

115 The particle size distributions were determined using a Laser diffraction particle size analyser  
116 (Malvern Mastersizer 2000®) (AFNOR, 2009) for the illitic material (Eslami, Rosin-Paumier,  
117 Abdallah, & Masrouri, 2015) and a wetting sieve method for the Plaisir loam. For the  
118 Jossigny and Xeuilley loams, the particle size distribution curves were found in the literature  
119 (Fleureau & Inderto, 1993 and Blanck, Cuisinier, & Masrouri, 2011). The Proctor optimum  
120 water contents ( $w_{OPN}$ ) and maximum dry densities ( $\rho_{dmax}$ ) were obtained from the standard  
121 Proctor curve performed for each mixture (AFNOR, 1999b) (*Figure 1* and *Table 3*).

## 122 **2.2. Sample preparation**

123 Six test series were performed (*Table 5*). In the first series, the effect of the dry density was  
124 studied on an illitic soil (I) and a sand-illitic mixture (S+I). In the second series, the effect of  
125 water content was studied on the same soils (I and S+I). In the third series, the effect of  
126 particle size and mineralogy were evaluated for each soil. Then, the coupled effect of dry  
127 density and water content was analysed by measuring the thermal properties of five materials  
128 compacted at various water contents and dry densities using constant compaction energy (4<sup>th</sup>  
129 series). Then, the temperature effect was studied on PL, I and S+I by measuring the thermal  
130 properties of different points on a compaction curve at varying temperatures within the range  
131 of 1 to 70°C (5<sup>th</sup> series). Finally, the effect of cyclic temperature variations was studied on PL  
132 (6<sup>th</sup> series).

133 To prepare samples at the desired water content and dry density, powdered material was first  
134 mixed with water to reach the target water content and then packed into hermitic bags to  
135 homogenize over at least 24 h. Two types of samples were prepared. For the 1<sup>st</sup> and 2<sup>nd</sup> series,  
136 samples 70 mm in height and 35 mm in diameter were statically compacted. For the 3<sup>rd</sup>  
137 through 6<sup>th</sup> series, samples 116 mm in height and 152 mm in diameter were dynamically  
138 compacted in three layers in a CBR (Californian Bearing Ratio) mould. The standard Proctor

139 compaction energy was applied. The samples were then heated or cooled to different  
140 temperatures in a climatic chamber, and the thermal properties of each sample were measured.

### 141 **2.3. Thermal parameter measurements**

142 The thermal properties were measured using a *KD2 Pro* thermal properties analyser®. Two  
143 specific sensors were used: a dual-needle SH-1 and a single needle TR-1. The dual-probe SH-  
144 1 consists of two parallel probes (30 mm long and 1.3 mm diameter with 6 mm spacing). One  
145 of these probes comprises a thermistor, and the other comprises the heater element. This  
146 sensor measures thermal conductivity ( $\lambda$ ), thermal resistivity (R), thermal diffusivity ( $\alpha$ ) and  
147 volumetric heat capacity (C) by employing the dual needle heat pulse method. The single  
148 needle TR-1 (2.4 mm diameter and 100 mm long) measures only thermal conductivity ( $\lambda$ );  
149 this is used when  $\lambda$  is higher than  $2 \text{ W.m}^{-1}.\text{K}^{-1}$ . The measurement range and the precision of  
150 both sensors are summarized in *Table 5*.

151 To measure the thermal parameters of sample, the probe was covered by a thin layer of grease  
152 (Arctiv Silver® 5 – High-density polysynthetic silver thermal compound) and then was  
153 placed in the sample after soil drilling at the same diameter. In this case, the use of the grease  
154 is recommended to improve the contact between the sensor needle and the soil. A waiting  
155 time of 15 minutes was imposed before each test to reach an equilibrium temperature between  
156 the probe and the soil. The presented value is a mean value of 4 tests in different locations of  
157 the sample.

## 158 **3. Experimental results and discussion**

159 In the following sections, the experimental results and discussions for each series are  
160 presented successively.



161 **3.1. Dry density effect on thermal parameters (1<sup>st</sup> series)**

162 The effects of dry density on thermal parameters are studied on both illitic material (I) and a  
163 sand-illitic mixture (S+I). Illitic samples were prepared at an initial water content in the range  
164 of 28.8 to 33.4% and dry densities varying from 1.20 to 1.52 Mg/m<sup>3</sup>. Sand-illitic (S+I)  
165 samples were prepared at an initial water content (*w*) in the range of 16.9 to 20.4% and dry  
166 densities ( $\rho_d$ ) varying from 1.54 to 1.79 Mg/m<sup>3</sup>. The variations of water content and dry  
167 density were chosen in the same range of the standard Proctor curve for both materials. The  
168 samples were thus prepared at water contents and dry densities compatible with their use in  
169 geotechnical engineering. The real density ( $\rho_h$ ) of the samples can be determined from Eq. 1.

170 
$$\rho_h = (1 + w) \times \rho_d$$
  
(Eq. 1)

171 The results (*Figure 2a, b, c*) showed that the thermal conductivity, volumetric heat capacity  
172 and thermal diffusivity increased with increasing dry density for both materials regardless of  
173 the water content. Linear increases in  $\lambda$ , *C* and  $\alpha$  as functions of increasing dry density were  
174 shown, in agreement with literature.

175 The thermal diffusivities ( $\alpha=\lambda/C$ ) measured on the illitic samples were significantly lower  
176 than those of the sand-illitic samples.

177 **3.2. Water content effect on thermal properties (2<sup>nd</sup> series)**

178 The effect of water content on the thermal proprieties was showed by Tang (2005), Brandl  
179 (2006) and Barry-Macaulay et al. (2013). In *Figure 2*, the range variations of water content  
180 and dry density of I and S+I samples were the same as those in part 3.1. The enhancement of  
181 thermal conductivity as a function of water content increase was clearly observed (*Figure 2a*).  
182 *Figure 2b* showed that the volumetric heat capacity of both materials varied in the same  
183 range. The range variation of *w* has a negligible impact on the thermal diffusivity of both

184 materials. The results obtained in the 1<sup>st</sup> and 2<sup>nd</sup> series are in agreement with literature. They  
185 therefore validated the experimental procedure used in this study.

### 186 **3.3. Mineralogy and particle size effect on thermal properties (3<sup>rd</sup> series)**

187 The mineralogy of the sample has an effect on its thermal conductivity (Ekwue et al. 2006,  
188 Zhang et al., 2017). For example, Brigaud and Vasseur (1989) denoted that the  $\lambda$  of quartz  
189 ( $\lambda_{\text{quartz}} = 7.7 \text{ W.m}^{-1}.\text{K}^{-1}$ ) is higher than that of illite ( $\lambda_{\text{illite}} = 1.85 \text{ W.m}^{-1}.\text{K}^{-1}$ ). As a  
190 consequence, the addition of sand to illitic material provided a higher  $\lambda$  for the S+I samples in  
191 comparison with the illitic samples (*Figure 2a*).

### 192 **3.4. Coupled effect of water content and dry densities on thermal properties** 193 **(4<sup>th</sup> series)**

194 The coupled effect of water content and dry density was studied by measuring the thermal  
195 parameters of samples compacted on several points of the compaction curves of five materials  
196 (illite (I), illite+sand (S+I), Plaisir loam (PL), sand+Jossigny loam (S+JL), sand+Xeuilley  
197 loam (S+XL)) of varying size distribution and mineralogy. Measurements of thermal  
198 parameters ( $\lambda$ , C and  $\alpha$ ) were carried out on samples prepared with the same compaction  
199 energy.

200 The results (*Figure 3*) showed that the thermal conductivity of each material increased on the  
201 dry side of the compaction curve until reaching a maximum near the Proctor optimum. On the  
202 dry side of the compaction curve, the dry density and the water content both increased,  
203 resulting in an increase of  $\lambda$ . In contrast, on the wet side of the compaction curve, the  
204 evolutions are different according to the sample mineralogy. For the silicious materials (S+I,  
205 PL, S+JL, S+XL),  $\lambda$  decreased, whereas for the silicate material (I),  $\lambda$  remained at its highest  
206 values. These evolutions are consistent with the physical properties of the studied samples. On  
207 the wet side of the compaction curve, the water content continues to increase, whereas the dry

208 density decreases. As the saturation rate remains approximately the same, the water molecules  
209 took the place of solid grains. As  $\lambda_{\text{quartz}}$  ( $7.7 \text{ W.m}^{-1}.\text{K}^{-1}$ ) is higher than  $\lambda_{\text{water}}$  ( $0.61 \text{ W.m}^{-1}.\text{K}^{-1}$ )  
210 (Brigaud & Vasseur, 1989), the thermal conductivity of samples containing quartz decreased  
211 quite quickly, whereas the thermal conductivity of samples containing silicates ( $\lambda_{\text{illite}} = 1.9$   
212  $\text{W.m}^{-1}.\text{K}^{-1}$ ) remained at an approximately constant value.

213 The volumetric heat capacity of soils increased on the dry side of the compaction curve until  
214 reaching a maximum near the Proctor optimum. Then, the values remained constant or  
215 decreased slightly. The variation range of the volumetric heat capacity was identical for the  
216 five materials studied.

217 The thermal diffusivity followed the same variation as the thermal conductivity in accordance  
218 with its definition ( $D=\lambda/C$ ). Consequently, the thermal diffusivities of sand-loam mixtures  
219 (S+JL and S+XL) were three times higher than that of the illitic soil.

### 220 **3.5. Combined effect of water content, dry density and temperature variations on** 221 **thermal properties (5<sup>th</sup> series)**

222 According to the potential use of compacted soils near a heat source or heat sink (energy  
223 storage, buried cables, or waste storage), the effect of temperature on the thermal properties  
224 was studied within a maximum temperature range of 1 to 70°C. Samples were prepared at  
225 various  $w$  and  $\rho_d$  under the same compaction energy (standard Proctor). Three materials were  
226 investigated: the illitic material (I, *Figure 4*), the sand-illitic soil mixture (S+I, *Figure 5*) and  
227 the Plaisir loam (PL, *Figure 7* and *Figure 8*). Thermal diffusivity measurements for the I  
228 samples were quite scattered due to their very low values compared with the measurement  
229 range (*Table 4*). In the studied temperature range, the main evolutions obtained in the  
230 previous part were observed for each material:

- 231 - thermal parameters reached their maximum values near the Proctor optimum;
- 232 - thermal parameters increased on the dry side of the compaction curve;

233 - thermal parameters remained at their maximal values on the wet side of the  
234 compaction curve for illitic samples; and

235 - thermal parameters decreased on the wet side of the compaction curve for the S+I and  
236 PL samples.

237 Following this general trend, variations were noticed according to the sample temperature. An  
238 extensive experimental study was carried out on the illitic material, which was expected to be  
239 the material most sensitive to temperature variation. The uncertainty of this method (10%) is  
240 presented with a double arrow for one point of each series (*Figure 4a, b and c*). The variation  
241 of  $\lambda$  in the temperature range of 1 to 40°C was within this uncertainty interval, but for 70°C  
242 results have clearly shown an increase of  $\lambda$  with increasing temperature. Measurements  
243 performed on S+I and PL over a maximal temperature range of 1–50°C confirmed this trend.  
244 The increase of thermal conductivity linked to the sample temperature was more important on  
245 the dry side than on the wet side of the compaction curve. This phenomenon is in addition to  
246 the increase of  $\lambda$  linked to the dilatation of the components (water and minerals) with  
247 increasing temperature.

248 In a saturated soil, the heat flux moves through solids and liquids by diffusion. Convection  
249 movements may aid the transfer, but the liquid convection may be limited, especially in low  
250 permeability materials. In an unsaturated soil, at low saturation rates, as is the case on the dry  
251 side of the compaction curve, the material contains solids, water and air. The thermal  
252 conductivity of air is very low unless it contains water vapour. The water vapour moves  
253 through the pores, increasing the thermal conductivity of the material. At higher temperatures,  
254 the air is able to reach higher moisture contents, which increases its participation in thermal  
255 conduction.

256 The impact of temperature variations on the volumetric heat capacity was not as clear as that  
257 on  $\lambda$ , especially for the I and S+I samples. *Figure 4b and 5b* do not show a clear trend for the

258 evolution of this parameter. The impact of temperature variations seemed to be below the  
259 measurement sensitivity. For PL samples, C measurements at 50°C were higher than values at  
260 20°C in the case of L1 samples (*Figure 8*). The thermal diffusivity increased with increasing  
261 temperature in accordance with the  $\lambda$  evolution (*Figure 4c* and *5c*).

### 262 **3.6. Cyclic temperature variation effect on thermal properties (6<sup>th</sup> series)**

263 Several samples of Plaisir loam were submitted to cyclic variations of temperature. Different  
264 cycles of 20/50°C (*Table 6*) were applied to the samples that were hermetically closed to keep  
265 w constant. The measurements were performed at various steps of the temperature  
266 programmes, as defined in *Figure 6*.

267 The experimental results showed that heating the samples increased the thermal conductivity  
268 and the volumetric heat capacity. These results confirmed the trends obtained in the previous  
269 part.

270 The measurements after 60 cycles showed that the **thermal conductivity**  $\lambda_{PL}$  at 20°C after the  
271 thermal cycles (C3) was lower than  $\lambda_{PL}$  at 50°C (C2). Nevertheless, the value of  $\lambda_{PL}$  at 20°C  
272 measured after the cycles (C3) was slightly higher than  $\lambda_{PL}$  at 20°C measured at the beginning  
273 of the test (C1) (*Figure 7*). The thermal conductivity reflects the capacity of a material to  
274 conduct a heat flux, this difference can be due to a change in the soil structure after several  
275 cycles.

276 Measurements of the **volumetric heat capacity** at 20°C (C3) remained very close to those  
277 obtained in test (C1) (*Figure 8*). The volumetric heat capacity reflects the ability of a material  
278 to store energy, it may be considered as the sum of the participation of soil different  
279 component. The ratio between solid, liquid and air did not vary in the sample and the  
280 volumetric heat capacity remained unchanged.

281 **4. Conclusions**

282 The effects of dry density, water content, mineralogy, size distribution and temperature on the  
283 thermal conductivity, volumetric heat capacity and thermal diffusivity of five materials were  
284 studied in the laboratory. In accordance with previous studies, the thermal parameters of the  
285 studied materials increased with increasing dry density and water content. The samples with  
286 wider granularity had a higher density and better solid contacts that improved their thermal  
287 conductivity. The effect of water content on thermal conductivity was clearly observed in  
288 loose materials, whereas in denser materials, the effect was negligible. The thermal  
289 conductivity of materials increased with increasing quartz percentage and the spread of the  
290 granulometric curve, whereas the volumetric heat capacity of materials seemed less sensitive  
291 to variations in the mineralogy and particle size. In the compacted soils, the thermal  
292 conductivity, the volumetric heat capacity and the diffusivity increased on the dry side of the  
293 compaction curve until reaching a maximum near the Proctor optimum.

294 The effect of temperature variation on the thermal properties was studied within a maximum  
295 temperature range of 1 to 70°C. The thermal conductivity and thermal diffusivity increased  
296 significantly on the dry side of the compaction curve and at high temperatures (illitic soil at  
297 70°C), while the effect of temperature on the specific heat capacity was not significant. The  
298 increase in thermal conductivity induced by temperature variation was more important on the  
299 dry side than on the wet side of the compaction curve due to the water vapour movement.  
300 Heating the samples increased the thermal properties, but this modification is partially  
301 reversible after several cycles for thermal conductivity and totally reversible for volumetric  
302 heat capacity.

303

304

305 **5. References:**

306 AFNOR. (1993). *NF P94-051 Sols: reconnaissance et essais; Détermination des limites*  
307 *d'Atterberg-Limite de liquidité à la coupelle-Limite de plasticité au rouleau* [Soil:  
308 Investigation and testing. Determination of Atterberg's limits. Liquid limit test using  
309 cassagrande apparatus. Plastic limit test on rolled thread] (p. 15). Paris: Association Française  
310 de Normalisation.

311 AFNOR. (1996). *NF P 94-048: Sols : Reconnaissance et Essais – Détermination de la teneur*  
312 *en carbonate –Méthode du calcimètre* (p.11). Paris: Association Française de Normalisation.

313 AFNOR. (1999a). *NF EN 933-9: Tests for geometrical properties of aggregates - Part 9:*  
314 *Assessment of fines-Methylene blue test* (p.12). Paris: Association Française de Normalisation.

315 AFNOR. (1999b). *NF P 94-093 Sols: Reconnaissance et essais Détermination des références*  
316 *de compactage d'un matériau. Essai Proctor Normal-Essai Proctor Modifié* [Soils:  
317 Investigation and testing. Determination of the compaction characteristics of a soil. Standard  
318 Proctor test. Modified Proctor test] (p. 18). Paris: Association Française de Normalisation.

319 AFNOR. (2009). *ISO 13320: Particle size analysis–Laser diffraction methods* (p.60). Paris:  
320 Association Française de Normalisation.

321 Abu-Hamdeh, N.H. (2001). Measurement of the Thermal Conductivity of Sandy Loam and  
322 Clay Loam Soils using Single and Dual Probes. *Journal of Agricultural Engineering*  
323 *Research*, 80(2), 209–216.

324 Abu-Hamdeh, N.H. (2003). Thermal Properties of Soils as affected by Density and Water  
325 Content. *Biosystems Engineering*, 86(1), 97–102.

326 Abu-Hamdeh, N.H., & Reeder, R.C. (2000). Soil Thermal Conductivity: Effects of Density,  
327 Moisture, Salt Concentration, and Organic Matter. *Soil Science Society of America Journal*,  
328 64(4), 1285–1290.

329 Barry-Macaulay, D., Bouazza, A., Singh, R. M., Wang, B., & Ranjith, P. G. (2013). Thermal  
330 conductivity of soils and rocks from the Melbourne (Australia) region. *Engineering Geology*,  
331 164, 131–138.

332 Blanck, G., Cuisinier, O., & Masrouri, F. (2011, September). *Effet d'un traitement non*  
333 *traditionnel acide sur le comportement mécanique de trois limons*. 20<sup>ème</sup> Congrès Français de  
334 Mécanique, Besançon, France.

335 Boukelia, A. (2016). *Modélisation physique et numérique des géo-structures énergétiques*.  
336 (PhD thesis). Université de Lorraine, Nancy, France.

337 Brandl, H. (2006). Energy foundations and other thermo-active ground structures.  
338 *Géotechnique*, 56(2), 81–122.

339 Brigaud, F., & Vasseur, G. (1989). Mineralogy, porosity and fluid control on thermal  
340 conductivity of sedimentary rocks. *Geophysical Journal International*, 98, 525–542.

341 Dong, Y., McCartney, J.S. & Lu, N. (2015). Critical Review of Thermal Conductivity Models  
342 for Unsaturated Soils. *Geotechnical and Geological Engineering*, 33(2), 207-221.

343 De Vries, D. A. (1963). Thermal properties of soils. *Physics of Plant Environment*. North-  
344 Holland, Amsterdam.

345 Ehdezi, P.K. (2012). *Enhancing Pavements for Thermal Applications*. (PhD thesis).  
346 University of Nottingham, Royaume-Uni.

347 Ekwue, E.I., Stone, R.J., & Bhagwat, D. (2006). Thermal Conductivity of Some Compacted  
348 Trinidadian Soils as affected by Peat Content. *Biosystems Engineering*, 94, 461–469.

349 Eslami, H., Rosin-Paumier, S., Abdallah, A., & Masrouri, F. (2014). Impact of temperature  
350 variation on penetration test parameters in compacted soils. *European Journal of*  
351 *Environmental and Civil Engineering*. doi: 10.1080/19648189.2014.960952.

352 Farouki, O.T. (1981). Thermal properties of soils. Monograph 81-1. *U.S. Army Cold Regions*  
353 *Research and Engineering Laboratory*, Hanover, New Hampshire, USA.



354 Fleureau, J.M, & Indarto. (1993). Comportement du limon de Jossigny remanié soumis à une  
355 pression interstitielle négative. *Revue française de géotechnique*, 62, 59–66.

356 Giordano, N., Comina, C., Mandrone, G., & Cagni, A. (2016). Borehole thermal energy  
357 storage (BTES). First results from the injection phase of a living lab in Torino (NW Italy).  
358 *Renewable Energy*, 86, 993–1008.

359 Hanna, M.A., Chikhani, A.Y., & Salama, M.M.A. (1993). Thermal analysis of power cables  
360 in multi-layered soil. Part 1: Theoretical model. *IEEE Transactions on Power Delivery*, 8(3),  
361 761–771.

362 Hiraiwa, Y., & Kasubuchi, T. (2000). Temperature dependence of thermal conductivity of soil  
363 over a wide range of temperature (5-75°C). *European Journal of Soil Science*, 51(2), 211–  
364 218.

365 Johansen, O. (1977). Thermal conductivity of soils. *U.S. Army Cold Regions Research and*  
366 *Engineering Laboratory*, Hanover, New Hampshire, USA.

367 Kersten, M.S. (1949). *Thermal properties of soils* (Report No. 28). University of Minnesota:  
368 Retrieved from the University of Minnesota Digital Conservancy,  
369 <http://purl.umn.edu/124271>.

370 De Lieto Vollaro, R., Fontana, L., & Vallati, A. (2011). Thermal analysis of underground  
371 electrical power cables buried in non-homogeneous soils. *Applied Thermal Engineering*,  
372 31(5), pp.772–778.

373 Navarro, L., De Gracia, A., Niall, D., Castell, A., Browne, M., McCormack, S.J.,... Cabeza,  
374 L.F. (2016). Thermal energy storage in building integrated thermal systems: A review. Part 2.  
375 Integration as passive system. *Renewable Energy*, 85, 1334–1356.

376 Pahud, D. ( 2002). Geothermal energy and heat storage. *SUPSI – DCT – LEEE Laboratorio di*  
377 *Energia, Ecologia ed Economia*.

378 Péron, H., Knellwolf, C., & Laloui, L. (2011). A method for the geotechnical design of heat  
379 exchanger piles. In H. Jie & D. E. Alzamora (Eds.), *Geo-Frontiers 2011: Advances in*  
380 *Geotechnical Engineering* (470–479). Dallas, TX: American Society of Civil Engineers.  
381 Geotechnical Special Publications 211.

382 Rutqvist, J., Wu, Y.-S., Tsang, C.-F., & Bodvarsson, G. (2002). A modeling approach for  
383 analysis of coupled multiphase fluid flow, heat transfer, and deformation in fractured porous  
384 rock. *International Journal of Rock Mechanics and Mining Sciences*, 39(4), 429–442.

385 Smits, K., Sakaki, T., Howington, S., Peters, J., & Illangasekare, T. (2013). Temperature  
386 dependence of thermal properties of sands across a wide range of temperatures (30-70°C).  
387 *Vadose Zone Journal*, 12 : doi 10.2136/vzj2012.0033.

388 Standard ASTM (2000). D5334 – 14: Standard test method for determination of thermal  
389 conductivity of soil and soft rock by thermal needle probe procedure (8p). West  
390 Conshohocken, PA www. ASTM. org: ASTM International.

391 Tang, A. (2005). *Effet de la température sur le comportement des barrières de confinement*.  
392 (PhD thesis). École Nationale des Ponts et Chaussées, Paris, France. Retrieved from  
393 <http://pastel.archives-ouvertes.fr/pastel-00001594/>

394 Zhang, T., Cai, G., Liu, S., & Puppala, A. J. (2017). Investigation on thermal characteristics  
395 and prediction models of soils. *International Journal of Heat and Mass Transfer*, 106, 1074-  
396 1086.

397 Zhao, D., Qian, X., Gu, X., Jajja, S.A. & Yang, R. (2016). Measurement Techniques for  
398 Thermal Conductivity and Interfacial Thermal Conductance of Bulk and Thin Film Materials.  
399 *Journal of Electronic Packaging*, 138(4), 040802, 64p.

400 *Table 1. Mineralogical composition of the raw materials*

Material	Ref.	Quartz	calcium carbonate	Feldspar	clay minerals	Others
Illitic soil	I	Traces	12% Calcite	Traces	77% Illite 10% Kaolinite	
Plaisir Loam	PL	81%	5% Calcite 7% Dolomite	3%	5%	
Jossigny Loam	JL	98%	Traces	1%	1%	
Xeuilley Loam	XL	83%	2%	3%	11%	1% Goethite
Hostun Sand	S	97.4%	Traces			2.6%

401

402

403

404 *Table 2. The characteristics of the studied materials*

Properties	Illitic soil I	Plaisir loam PL	Jossigny loam JL Fleureau & Inderto (1993)	Xeuilley loam XL Blanck et al. (2011)
<b>Grain size distribution</b>				
Passer - by 80 $\mu\text{m}$	100	41	80	95
Passer - by 2 $\mu\text{m}$	85	20	28	25
<b>Atterberg limits</b>				
Plastic limit (%)	34	20.6	16 - 19	28
Liquid limit (%)	65	27.3	37	37
Plasticity index	31	6.7	18 - 21	9
<b>Specific surface</b>				
MBV(g/100g)	5.41	1.85	-	3.1
<b>Carbonate content</b>				
CaCO <sub>3</sub>	-	0.8	-	1.3
<b>Proctor compaction</b>				
WOPN (%)	31.3	16	15.5	18.5
$\gamma_{\text{dmax}}/\gamma_{\text{w}}$	1.43	1.81	1.75	1.71
$\gamma_{\text{max}}/\gamma_{\text{w}}$	1.88	2.10	2.02	2.03
<b>Soil Class</b>				
GTR Classification	A3	A1	A2	A2
USCS Classification	MH	CL	CL	ML

405

406

407

408

409

410

411

412 *Table 3. Composition and parameters of the standard Proctor curve for the mixtures*

Mixture	Composition	WOPN (%)	$\rho_{dmax}$ (Mg/m <sup>3</sup> )	$\rho_{hOPN}$ (Mg/m <sup>3</sup> )
S+I	50% Hostun sand and 50% Illitic soil	18.6	1.71	2.03
S+JL	50% Hostun sand and 50% Jossigny Loam	13.6	1.89	2.15
S+XL	50% Hostun sand and 50% Xeuilley Loam	13.7	1.88	2.14

413

414

415

416

417

418 *Table 4. Performed tests as a function of material type*

Series	Variables	Materials				
		I	S+I	PL	S+JL	S+XL
1	$\gamma$	+	+			
2	w	+	+			
3	mineralogy and particle size	+	+	+		
4	w and $\gamma$	+	+	+	+	+
5	w and $\gamma$ and T	+	+	+		
6	w and $\gamma$ and T (cycle)			+		

419

420

421 *Table 5. Range and precision of sensors SH-1 and TR-1*

Sensor	Propriety	Measure range	Precision
TR-1	Thermal conductivity (W.m <sup>-1</sup> .K <sup>-1</sup> )	0.1 - 0.2	± 0.02
		0.2 - 4	± 10 %
SH-1	Thermal conductivity (W.m <sup>-1</sup> .K <sup>-1</sup> )	0.02 - 0.2	± 0.01
		0.2 - 2	± 10 %
SH-1	Thermal diffusivity (mm <sup>2</sup> /s)	0.1 - 1	± 10 %
SH-1	Volumetric heat capacity (MJ.m <sup>-3</sup> K <sup>-1</sup> )	0.5 - 4	± 10 %

422

423

424

425

426

427

428 *Table 4. Temperature programme applied on PL (6<sup>th</sup> series)*

Program	Stage 1		Stage 2		NB cycle
	T°C	Time	T°C	Time	
P1	20	9h	50	9h	60
P2	20	2h	50	4h	60
P3	20	9h	50	9h	4

429

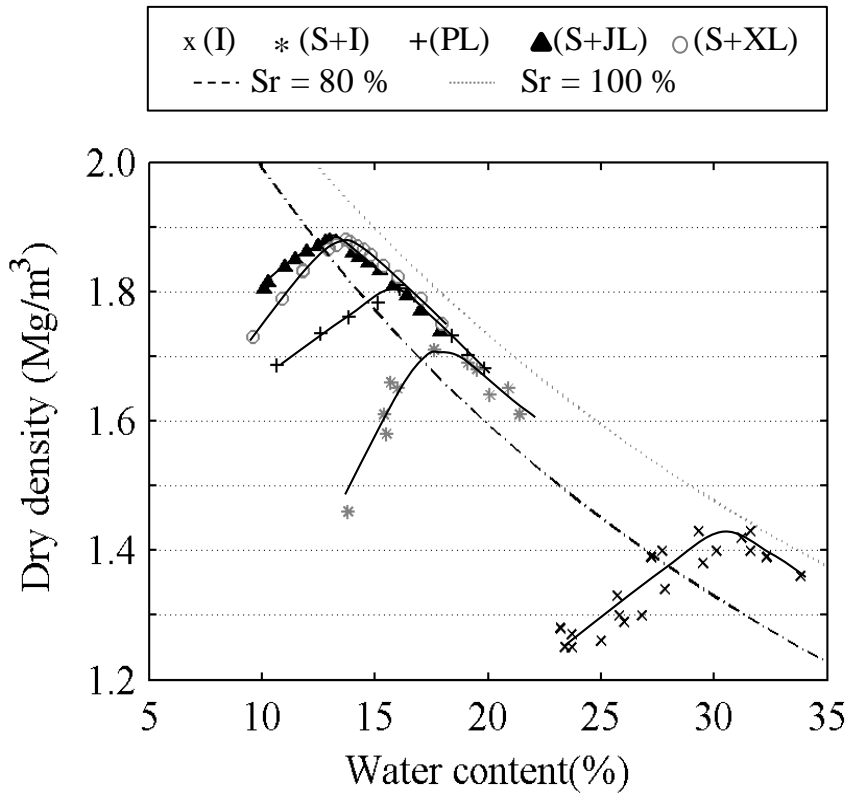
430

431

432

433





434

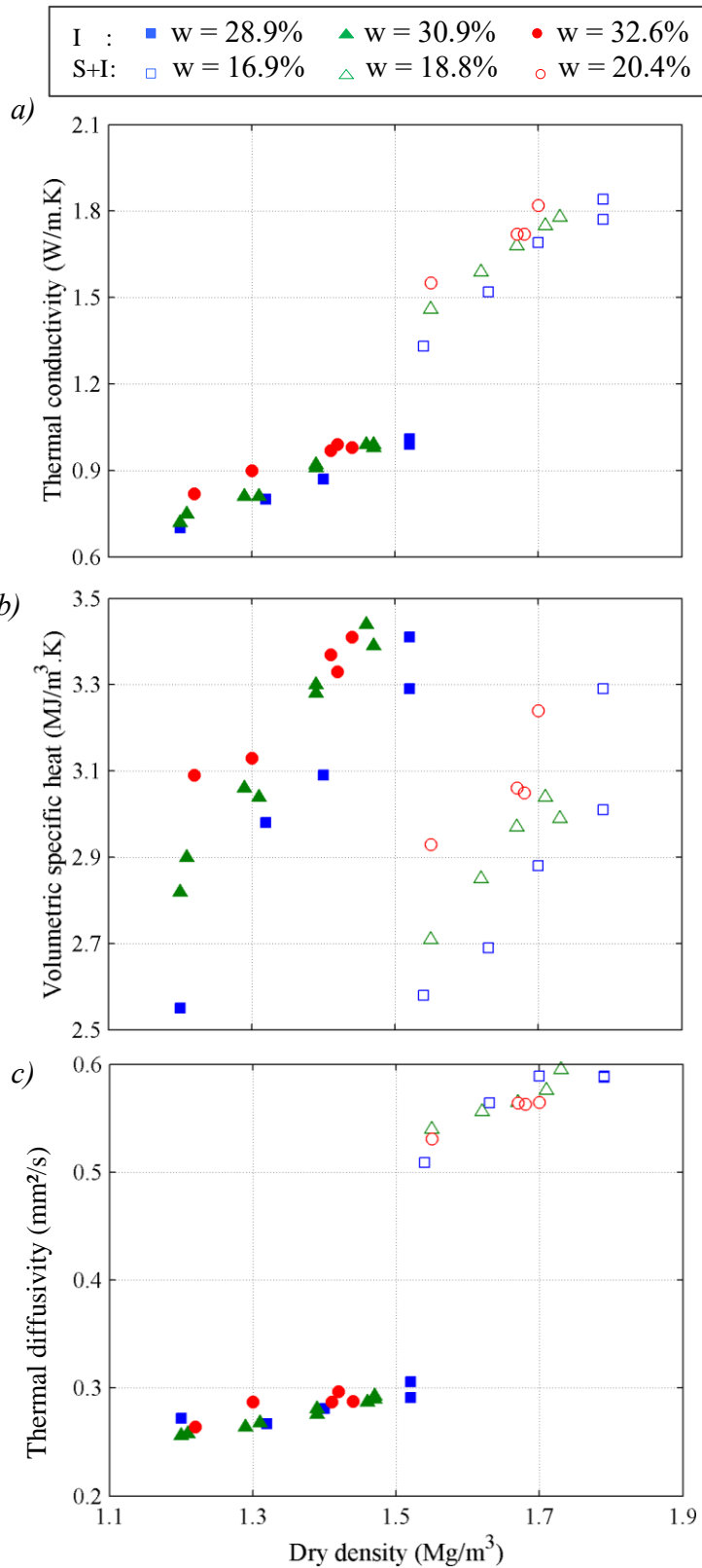
435 *Figure 1. Compaction curves of the studied materials.*

436

437

438

439

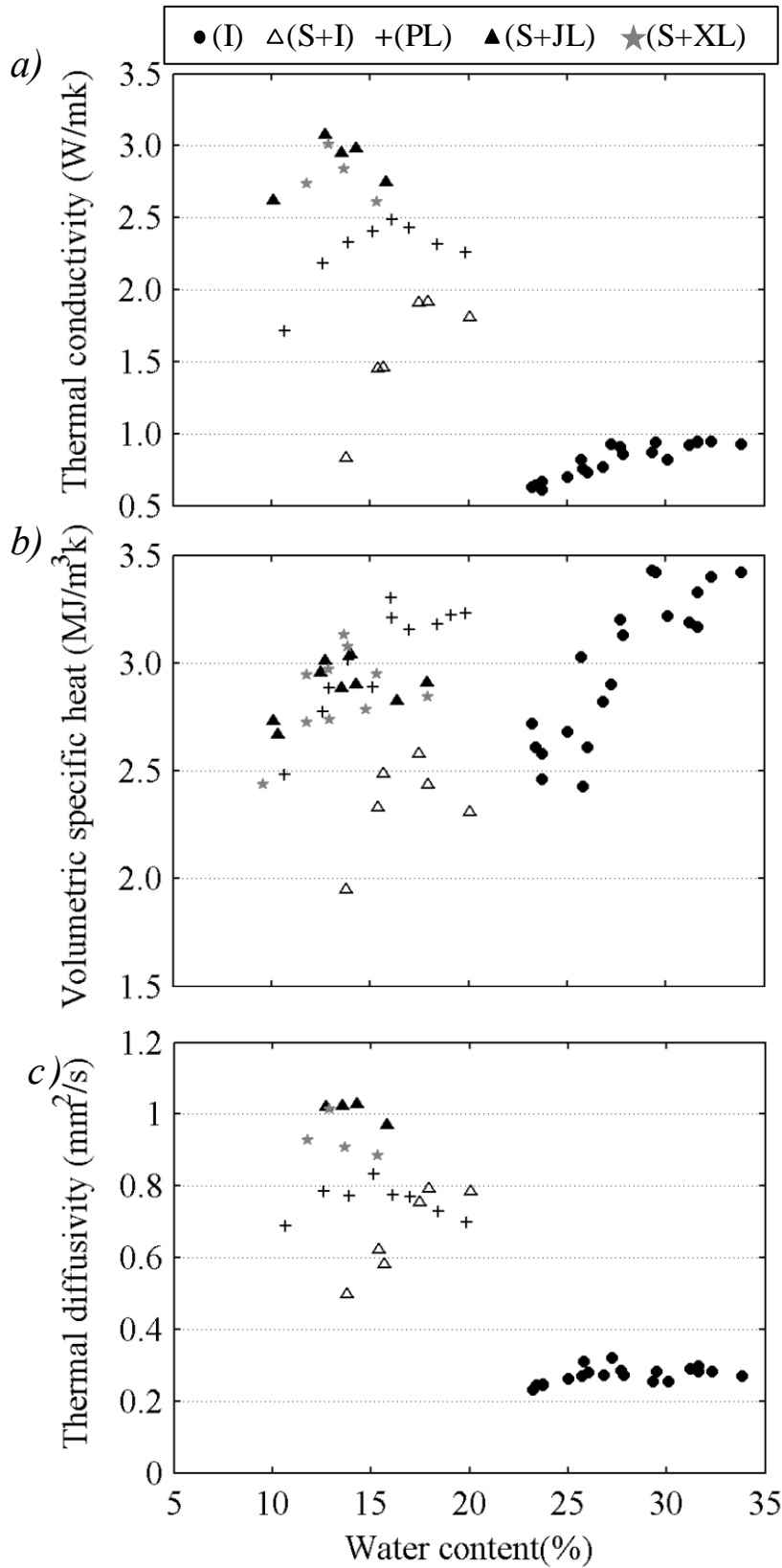


440

441 *Figure 2. Evolution of the (a) Thermal conductivity, (b) Volumetric heat capacity and (c)*

442 *Thermal diffusivity as a function of dry density at different water contents for the illitic*

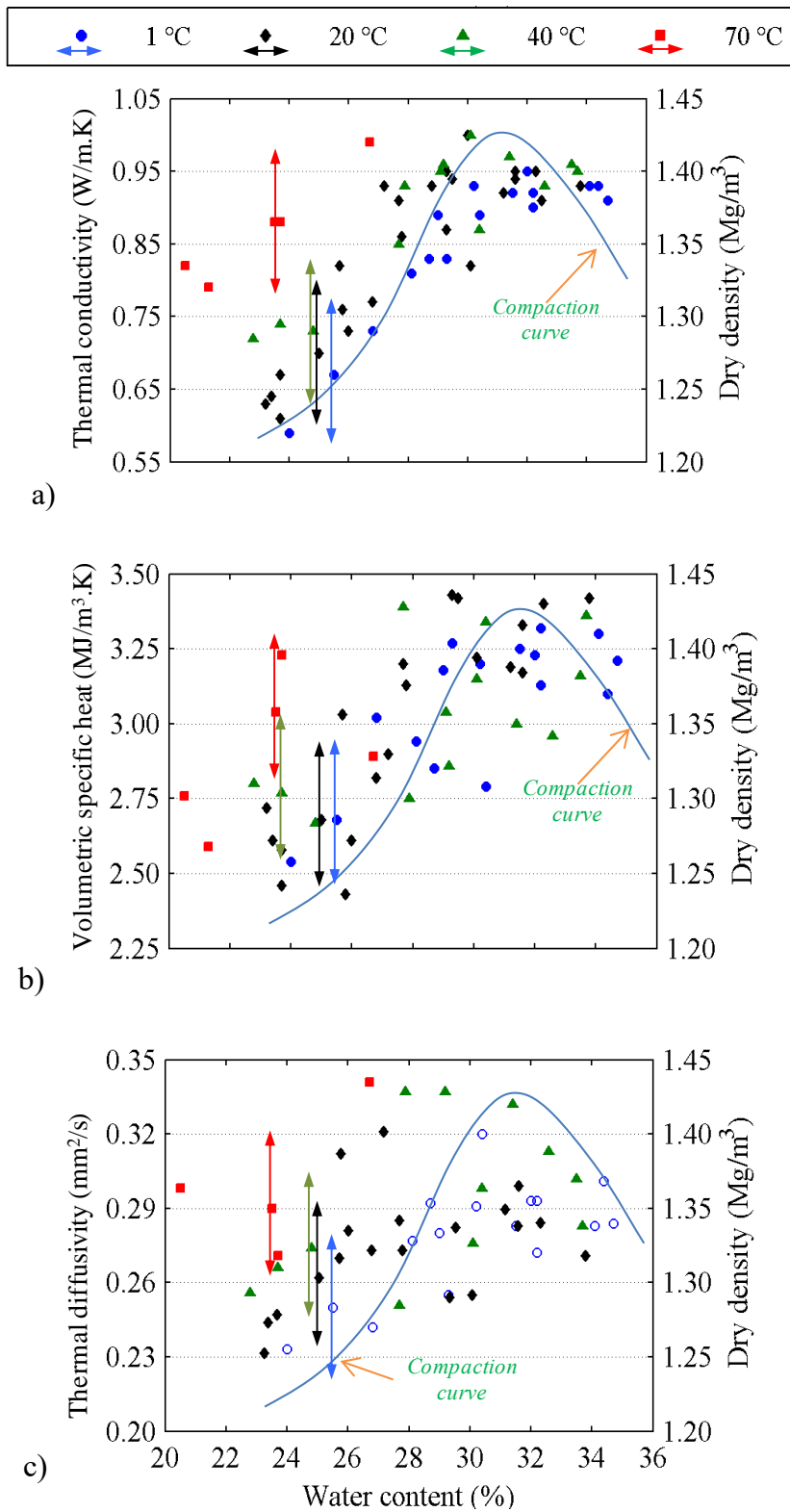
443 *material (I) and the sand-illitic material mixture (S+I) (1<sup>st</sup> and 2<sup>nd</sup> series).*



444

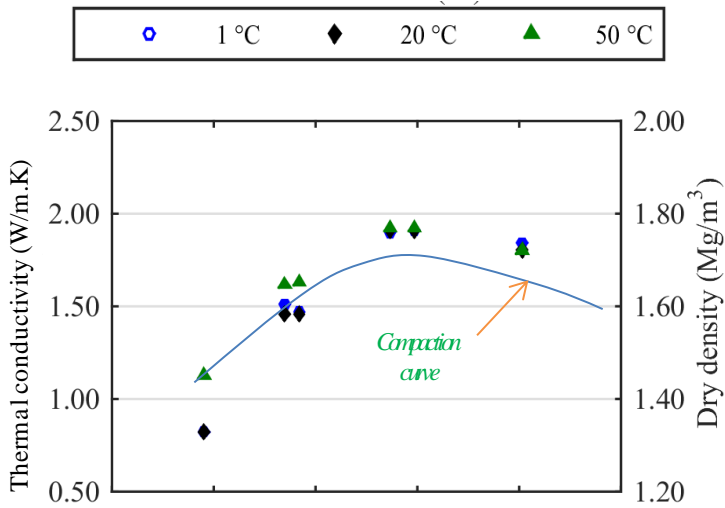
445 *Figure 3. (a) Thermal conductivity, (b) Volumetric heat capacity and (c) thermal diffusivity as*

446 *a function of water content and dry density of materials (4<sup>th</sup> series).*

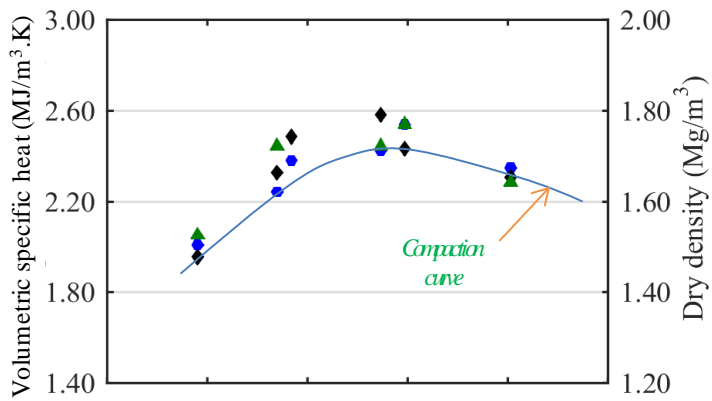


447  
448

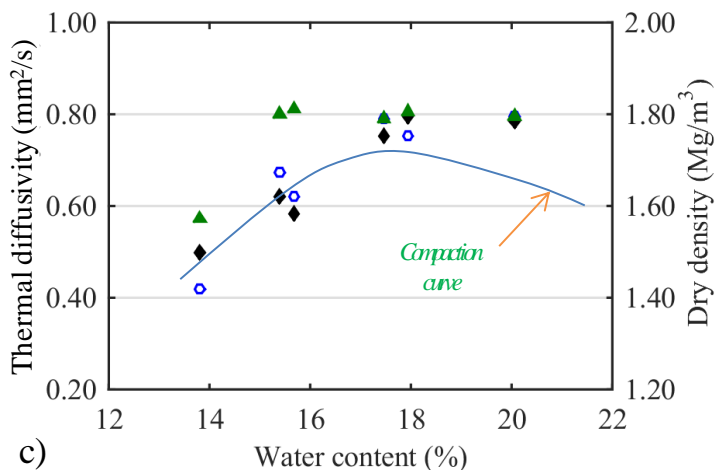
449 *Figure 4. Evolution of the thermal properties of the illitic soil (I) according to the*  
 450 *temperature and uncertainty (double arrow) : (a) Thermal conductivity, (b) Volumetric heat*  
 451 *capacity and (c) Thermal diffusivity (5<sup>th</sup> series).*



a)



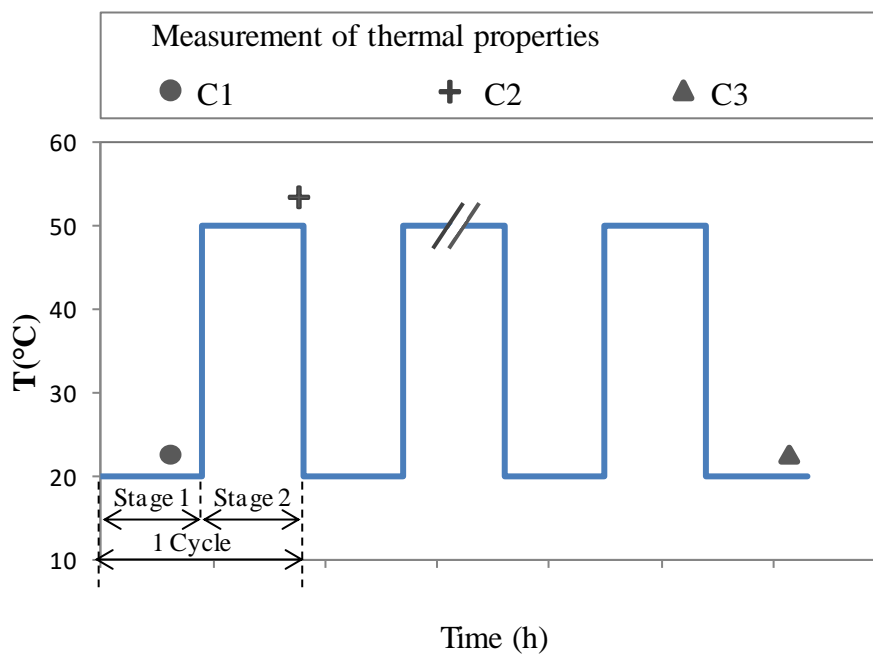
b)



c)

452  
 453 *Figure 5. Evolution of the thermal properties of the sand-illitic soil mixture (S+I) according*  
 454 *to the temperature: (a) Thermal conductivity, (b) Volumetric heat capacity and (c) Thermal*  
 455 *diffusivity (5<sup>th</sup> series).*

456



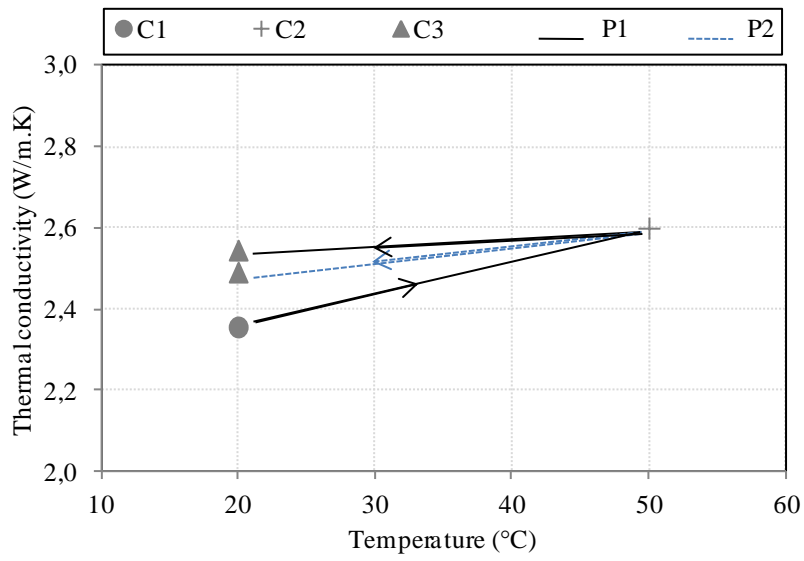
457

458 *Figure 6. The chronology of measurements as a function of cyclic temperature variation*

459 *applied to the PL samples (6<sup>th</sup> series).*

460

461

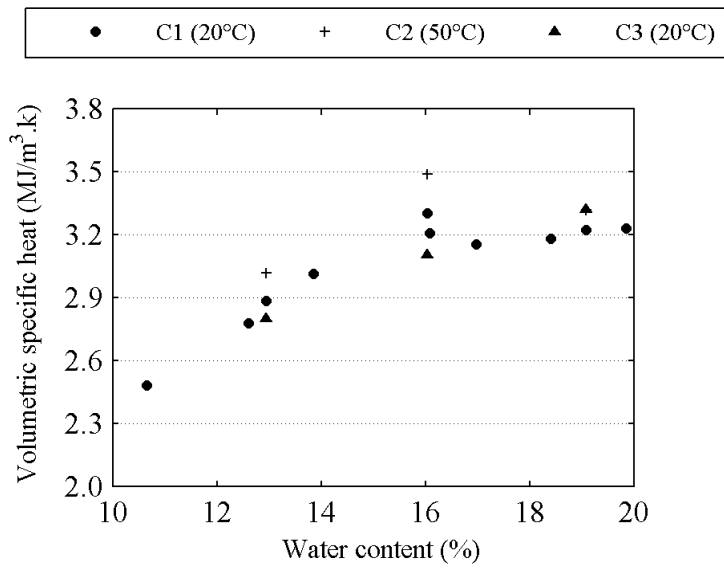


462

463 *Figure 7. Warming effect on thermal conductivity of PL (P1, P2, 6<sup>th</sup> series).*

464

465



466

467 *Figure 8. Warming effect on volumetric heat capacity of PL (P3, 6<sup>th</sup> series).*